SERBIAN JOURNAL OF ELECTRICAL ENGINEERING
Vol. 17, No. 3, October 2020, 313-336

UDC: 621.314/316:004.42 **DOI: https://doi.org/10.2298/SJEE2003313N**

An Enhanced Exponential Reaching Law Based Sliding Mode Control Strategy for a Three Phase UPS System

Venkatesh Nayak[1], Satish Kumar Gudey[1]

Abstract: UPS is used to deliver a high quality sinusoidal waveform to consumers without any interruptions. This work proposes an Enhanced Exponential Reaching Law (EERL) based Sliding Mode Control (SMC) for a three- phase UPS 30 kVA system used in industrial Applications. The work presents the application of proposed controller on the rectifier side as well as on the inverter side feeding a linear and/or a nonlinear load. Mathematical models of the three phase rectifier (AC/DC) and three phase inverter (DC/AC) are derived. Frequency response characteristics are plotted to observe the system stability using state feedback approach. A DC/DC buck/boost converter is utilised for charging and discharging of battery which acts as a secondary power source for the UPS to feed critical loads. It also maintains power balance. The design of SMC, HOSMC and EERL-SMC are presented. The EERL based SMC is used in this work to obtain a pure sinusoidal waveform with less settling time compared to a conventional SMC. It is robust against sudden changes in load and is more efficient compared to SMC and higher order sliding mode controller (HOSMC). Using EERL, chattering phenomenon can be very much reduced with less steady state error. Chattering is observed through phase plane plots in this paper. The system is presented with both linear and nonlinear loads. A comparison is brought with respect to a classical SMC and a higher order SMC (super twisting algorithm) for a UPS system. EERL-SMC performs better in terms of pure sinusoidal waveform, good tracking, less settling time (4ms) and less steady state error (1.74%) with low THD (0.12%). It can be an alternative to a HOSMC. Simulation studies are presented in PSCAD/EMTDC version 4.6. The system stability conditions are analysed from frequency response plots obtained through MATLAB R2012b platform.

Keywords: Battery, Chattering, Enhanced Exponential Reaching Law (EERL), Sliding Mode Controller (SMC), Super Twisting Algorithm, buck/boost converter, Uninterruptible Power Supply (UPS).

[1]Department of Electrical and Electronics Engineering, Gayatri Vidya Parishad College of Engineering (Autonomous), Visakhapatnam, Andhra Pradesh, India-530041;
Emails: venky.naik3@gmail.com , satishgudey5@gvpce.ac.in

1 Introduction

Nowadays every end user needs a good quality of power supply without any interruptions. Uninterruptible Power Supply (UPS) is one such device used to deliver a high quality sinusoidal waveform to consumers without any interruptions. UPS is designed with a Voltage Source Converter (VSC) for AC/DC/AC power conversion and a DC link battery for energy storage. The output of the Voltage Source Inverter (VSI) is a sine wave with required magnitude and phase for different critical load applications. The main important applications of UPS include industrial plants, communication systems, hospital and military system which are critical loads. There is always a need to design new control strategy for UPS system to improve the quality of inverter output voltage waveforms [1]. There are many controllers starting form hysteresis current controllers to model predictive controllers available in the literature [2]. But Sliding Mode Controller (SMC) controller is a robust and a dynamic controller compared to any other controllers [1]. It has better output voltage reference tracking capability. Much literature is available on SMC, its advantages and disadvantages for a power electronics system [3].

Chattering is defined as the operation of the system at very high frequencies which creates noises in the system. A Higher order SMC is suitable for elimination of this chattering phenomenon [4]. Many algorithms like twisting, super twisting and suboptimal, terminal, fast terminal SMC are available in the literature. These controllers are basically used to move any state variable in the state space to origin making the system stable. In doing so, the chattering and settling time are reduced or eliminated which was present in the classical SMC [4].

A UPS operates with a Voltage Source Converter (VSC) for AC/DC/AC power conversion and a DC link battery for energy storage [5]. Therefore, a suitable control strategy is essential for an UPS system to deliver reliable power supply for such applications. An efficient & effective control method always enhances the system output power. Power Electronic converters are inherently VSS in nature and hence SMC is suitable for an UPS system [6].

In this work, first a classical SMC is designed to control the desired sinusoidal output voltage using an inner current control loop and an outer voltage control loop as a dual-control scheme. The objective is to obtain a pure sine wave with less harmonic content in output voltage waveform. It is observed that the classical SMC has a major drawback in terms of high switching frequency oscillations around the sliding surface i.e. chattering phenomenon [6]. To alleviate chattering in this work, secondly a Higher Order Sliding Mode Controller (HOSMC) by name Super Twisting Algorithm (STA) is also proposed [5]. These operate on the derivatives of state variables instead of the state variable itself which reduces the use of number of sensors in the control

system [4]. A saturation sign function of sliding surface is used to avoid chattering in this work [6].

The proposed EERL-SMC in this work is a suitable alternative for HOSMC. In literature, reaching laws can be classified as three types i.e. Conventional, Power rate and Exponential reaching law [7]. An Enhanced Exponential reaching Law based on SMC is proposed in this work which overcomes the drawbacks of SMC, HOSMC. The system returns to the stable state with less settling time. Also, the results obtained are nearer to a sine wave with less THD. A comparison between the proposed algorithm w. r. t SMC and HOSMC encourages the researchers to explore the possibilities of adapting this new algorithm to a three phase UPS system.

The analysis not only delivers the use of EERL-SMC but also overcomes the merits and demerits in the classical and Higher order SMC through extensive Simulation and Mathematical models. This is for the first time that the authors have presented the use of classical SMC, HOSMC and EERL-SMC for a three phase UPS system both on the input (rectifier) and output side (inverter) of the UPS system. The parameters used to observe the performance of the proposed controller are the steady state error, settling time through phase plane portraits and total harmonic distortion (THD, battery state of charge and chattering. For hardware implementation, the number of sensors required is also studied. Finally, to evaluate the proposed control algorithm EERL-SMC for a three phase UPS in an Industrial Application.

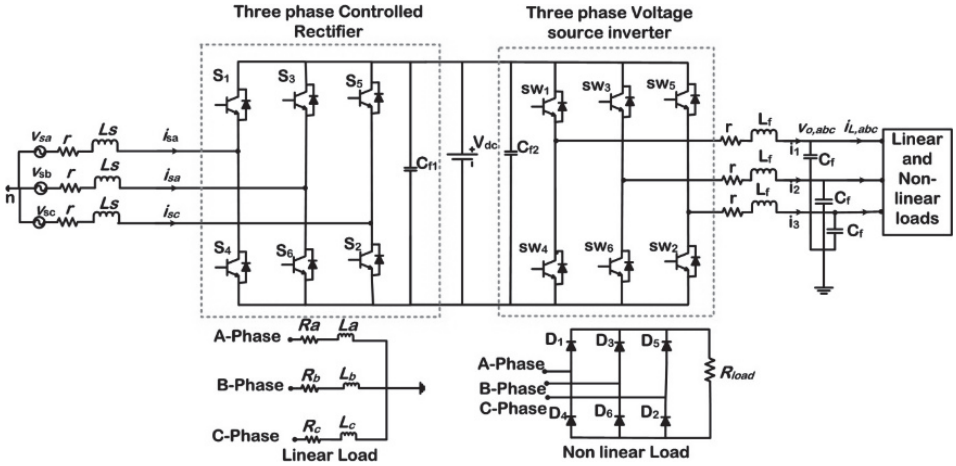

Fig. 1 − *Structure of VSC in UPS configuration.*

A three phase UPS structure feeding linear and non-linear loads shown in Fig. 1 is the system considered in this work. In Section 2 controlled rectifier and voltage source inverter state space models are presented. The stability of the system is studied using state feedback approach through frequency response

characteristics. In Section 3 control methodologies of UPS system i.e. SMC, HOSMC and Proposed Controller i.e. EERL-SMC are presented and section 4 includes DC/DC Buck-Boost converter control scheme. Section 5 includes results and discussions from the work.

2 Mathematical Modeling of Three Phase Rectifier and VSI

The power circuit of a 3-Ø UPS system with DC-DC buck/boost converter for energy storage system is shown in Fig. 2. The system consists of a three phase fully controlled rectifier for AC/DC power conversion. The DC energy storage battery bank is connected to DC-Link voltage across the capacitor C_f through DC- DC buck/boost converter for charging and discharging the battery bank. It is operated in such a way that the battery supplies the stored energy during grid power interruption. On the other side of the UPS, three phase voltage source inverter (VSI) is connected to different types of critical loads through passive *LC* filters. The loads taken are three phase balanced linear *RL* and non-linear three phase diode bridge rectifier loads (DBR) [8].

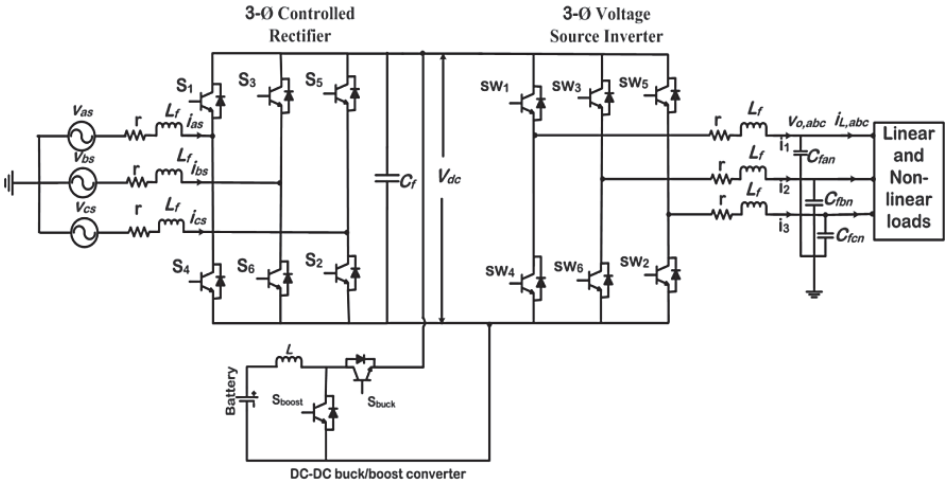

Fig. 2 – *Power circuit of a 3-Ø UPS system with DC-DC buck/boost converter for energy storage.*

2.1 Model of Three Phase Controlled Rectifier

KVL is applied to input side of the three phase control rectifier [9] to determine the input source voltages equation (1). The derivatives of input source currents of controlled rectifier are obtained because these currents are taken as state variables (2), where n=a, b, c,

$$v_{sn} = i_{sn} r + L_f \frac{\mathrm{d}i_{sn}}{\mathrm{d}t} + u_n , \tag{1}$$

$$\frac{\mathrm{d}i_{sn}}{\mathrm{d}t}=\frac{1}{L_f}\left[v_{sn}-i_{sn}r-u_n\right], \tag{2}$$

(3) represents the derivative of the output dc voltage of the rectifier

$$\frac{\mathrm{d}V_{dc}}{\mathrm{d}t}=\frac{u_a i_{sa}+u_b i_{sb}+u_c i_{sc}}{c_f V_{dc}}-\frac{I_{dc}}{c_f}. \tag{3}$$

A synchronously rotating reference frame transformation is used to express the system equations in a *d-q* frame which is more convenient for control design [10]

$$\begin{bmatrix} d \\ q \\ 0 \end{bmatrix}=\frac{2}{3}\begin{bmatrix} \cos\theta & \cos\left(\theta-\frac{2\pi}{3}\right) & \cos\left(\theta+\frac{2\pi}{3}\right) \\ \sin\theta & \sin\left(\theta-\frac{2\pi}{3}\right) & \sin\left(\theta-\frac{2\pi}{3}\right) \\ \frac{1}{2} & \frac{1}{2} & \frac{1}{2} \end{bmatrix}\begin{bmatrix} a \\ b \\ c \end{bmatrix}. \tag{4}$$

The state vector *x* is represented with the state variables chosen as

$$x^{\mathrm{T}}=\begin{pmatrix} i_d & i_q & V_{dc} \end{pmatrix}. \tag{5}$$

The obtained state space model is represented as (6)

$$\begin{bmatrix} \dot{i}_d \\ \dot{i}_q \\ \dot{V}_{dc} \end{bmatrix}=\begin{bmatrix} -\frac{r}{L_f} & -\omega & 0 \\ \omega & -\frac{r}{L_f} & 0 \\ 0 & 0 & -\frac{1}{R_{Load}\times C_f} \end{bmatrix}\begin{bmatrix} i_d \\ i_q \\ V_{dc} \end{bmatrix}+\begin{bmatrix} \frac{v_d}{L} \\ \frac{v_q}{L} \\ 0 \end{bmatrix}u. \tag{6}$$

Using state feedback approach**,** the stability of the system is observed through bode plot [11]. The direct and quadrature rotating axis currents i_d and i_q and output DC voltage v_{dc} of the rectifier are considered as state variables, the output equation is given by $y = Cx$, where C = [1 1 1].

The corresponding open loop transfer function is given in (7)

$$G_{i_d,i_q,v_{dc}}(s)=\frac{6.76\times10^{-5}s^2+4.5\times10^{8}s+5.63\times10^{10}}{s^3+1167s^2+5.15\times10^{5}s+5.81\times10^{7}}. \tag{7}$$

The phase margin is 90º and gain margin is infinity which means the system is said to be stable with the desired state variables.

2.2 Model of Three Phase Voltage Source Inverter (VSI)

A three phase VSI circuit consists of *LC* filter to reduce harmonics present in the output voltage of VSI which drives a linear load i.e. *RL* load [12].

Voltage equations for state variables (v_{an}, v_{bn}, v_{cn}) are as shown in (8)

$$\frac{\mathrm{d}v_{jn}}{\mathrm{d}t} = \frac{i_k}{C_{fjn}} - \left(\frac{1}{Z_j \times C_{jn}}\right) v_{jn}. \tag{8}$$

Inductor Current equations for state variables i_k, $k = 1, 2, 3$ and $j = a, b, c$

$$\frac{\mathrm{d}i_k}{\mathrm{d}t} = \frac{v_{dc}}{L_{jf}} - \frac{r}{L_{jf}} i_k - \frac{v_{jn}}{L_{jf}}. \tag{9}$$

The chosen state variables are:

$$x^{\mathrm{T}} = \begin{pmatrix} v_{an} & v_{bn} & v_{cn} & i_1 & i_2 & i_3 \end{pmatrix}. \tag{10}$$

The *abc* model is transformed into the αβ co-ordinate system by using Clark's transformation method. The transformation matrix is adopted as in [13]

$$\begin{pmatrix} \dot{v}_{an} \\ \dot{v}_{bn} \\ \dot{v}_{cn} \\ \dot{i}_1 \\ \dot{i}_2 \\ \dot{i}_3 \end{pmatrix} = \begin{pmatrix} \frac{-1}{Z_a \times C_{fan}} & 0 & 0 & \frac{1}{C_{fan}} & 0 & 0 \\ 0 & \frac{-1}{Z_b \times C_{fbn}} & 0 & 0 & \frac{1}{C_{fbn}} & 0 \\ 0 & 0 & \frac{-1}{Z_c \times C_{fcn}} & 0 & 0 & \frac{1}{C_{fcn}} \\ \frac{-1}{L_{af}} & 0 & 0 & \frac{-r}{L_{af}} & 0 & 0 \\ 0 & \frac{-1}{L_{bf}} & 0 & 0 & \frac{-r}{L_{bf}} & 0 \\ 0 & 0 & \frac{-1}{L_{cf}} & 0 & 0 & \frac{-r}{L_{cf}} \end{pmatrix} \begin{pmatrix} v_{an} \\ v_{bn} \\ v_{cn} \\ i_1 \\ i_2 \\ i_3 \end{pmatrix} + \begin{pmatrix} 0 \\ 0 \\ 0 \\ \frac{V_{dc}}{L_{af}} \\ \frac{V_{dc}}{L_{bf}} \\ \frac{V_{dc}}{L_{cf}} \end{pmatrix} \begin{pmatrix} u_a \\ u_b \\ u_c \end{pmatrix}, \tag{11}$$

$$\begin{pmatrix} \alpha \\ \beta \end{pmatrix} = \sqrt{\frac{2}{3}} \begin{pmatrix} 1 & -\frac{1}{2} & -\frac{1}{2} \\ 0 & \frac{\sqrt{3}}{2} & -\frac{\sqrt{3}}{2} \end{pmatrix} \begin{pmatrix} a \\ b \\ c \end{pmatrix}. \tag{12}$$

VSI in the stationary reference frame is derived as (13)

$$\begin{pmatrix} \dot{v}_{mn} \\ \dot{i}_m \end{pmatrix} = \begin{pmatrix} \frac{-1}{Z_m C_{fmn}} & \frac{1}{C_{fmn}} \\ \frac{-1}{L_{mf}} & \frac{-r}{L_{mf}} \end{pmatrix} \begin{pmatrix} v_{mn} \\ i_m \end{pmatrix} + \begin{pmatrix} 0 \\ \frac{V_{dc}}{2L_{mf}} \end{pmatrix} u_m. \tag{13}$$

Assuming $m = \alpha, \beta$. Open loop transfer function can be derived from the state space model (11) for the VSI circuit. The corresponding open loop transfer function is given (14)

$$G_{vi}(s) = \frac{1\times10^{5}s + 1.72\times10^{11}}{s^{2} + 1.67\times10^{6}s + 2.77\times10^{8}}. \quad (14)$$

Phase margin is 87.8° and gain margin is infinity. Both values are positive, hence the system is said to be stable.

2.3 Summary of the characteristics of VSC in UPS System

It is clearly observed that, in three phase rectifier direct and quadrature axis currents and output voltage are to be controlled so that system exhibits desired response with better stability. In three phase VSI, output phase voltages and filter inductor currents are to be controlled, so that system exhibits better stability margins.

Table 1

Summary of Frequency Response Characteristics.

State Variables	Phase Margin (dB)	Gain Margin (dB)	Stability
$v_{\alpha n}$, i_{α} (for VSI)	89.9°	Infinity	Stable
i_d, i_q, v_{dc} (For rectifier)	90°	Infinity	Stable

3 Control Methodologies for UPS System

3.1 Classical Sliding Mode Controller (SMC)

SMC is a non-linear control technique and is an alternative to the linear techniques. The geometrical locus having some boundaries is called sliding surface (*S)* [14]. The foremost step to design the controller is appropriate selection of sliding surface [15].

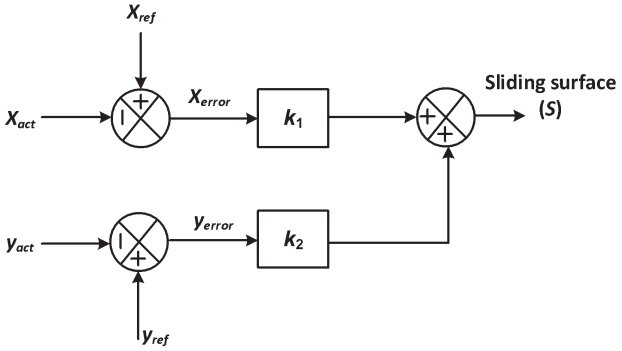

Fig. 3 – *Control diagram of a classical SMC.*

Fig. 3 shows the block diagram of an SMC used in this work. It is the sum of the two state variable errors with product of sliding coefficients gains (k_1 and k_2), respectively,

$$s = k_1 x_{error} + k_2 y_{error}\,, \tag{15}$$

where k_1 and k_2 are sliding coefficients of controller. The errors (x and y) of system depends upon the ratio of sliding coefficients, i.e., $\tau = k_2/k_1$ s. Its value is chosen smaller so as to reach the origin in less time.

3.1.1 SMC for Three-Phase Controlled Rectifier Circuit

Equations (16) and (17) refer to the outer voltage loop of controlled rectifier [16]. (17) represents PI controller which acts like a current regulator

$$s_{dc} = v_{dcref} - v_{dc}\,, \tag{16}$$

$$i_{dref} = k_1(k_{pdc} s_{dc} + k_{idc} \int s_{dc}\, \mathrm{d}t)\,. \tag{17}$$

Using (16) and (17) design of inner current loop is obtained as (18) and (19)

$$u_d = v_d - \omega L i_q - k_2(k_{pd} s_d + k_{id} \int s_d\, \mathrm{d}t)\,, \tag{18}$$

$$u_q = v_q - \omega L i_d - k_3(k_{pq} s_q + k_{iq} \int s_q\, \mathrm{d}t)\,. \tag{19}$$

The decoupling feed forward method is used in SMC current controller.

3.1.2 SMC for Three Phase VSI Circuit

Equations (23) and (24) derive the SMC for a VSI using state variables v_α and v_β,

$$v_{\alpha ref} = v_m \sin \omega t\,, \tag{23}$$

$$v_{\beta ref} = v_m \sin(\omega t + 90)\,. \tag{24}$$

In stationary reference frame the phase angle difference between $\alpha\beta$ is 90º. Magnitude of input AC voltage is $v_m = 1.414 v_{rms}$ and $v_{l-l} = 415$ V (rms). Equations (25) and (26) represent the reference current generation for the SMC

$$i_{\alpha ref} = v_{\alpha error}\left(k_{p\alpha} + \frac{k_{i\alpha}}{s}\right), \tag{25}$$

$$i_{\beta ref} = v_{\beta error}\left(k_{p\beta} + \frac{k_{i\beta}}{s}\right). \tag{26}$$

Now sliding surface is written as (27) and (28)

$$s_\alpha = (v_{\alpha error} \times k_1) + (i_{\alpha error} \times k_2)\,, \tag{27}$$

$$s_\beta = (v_{\beta error} \times k_1) + (i_{\beta error} \times k_2)\,. \tag{28}$$

The sliding coefficients are set to k_1= 280 and k_2= 25 for a time constant of T = 9 ms in this work. The generating sliding surfaces (s) is compared with a triangular carrier signal to generate switching gate pulses to VSI.

$$S(t) = \begin{cases} +1 & \text{for} \quad S(t) > 0, \\ -1 & \text{for} \quad S(t) < 0. \end{cases} \tag{29}$$

The stability condition is given by [17]

$$S\dot{S} < 0\,. \tag{30}$$

This design process is used in this work for generating a pure sine voltage waveform in a UPS system using SMC which feed different loads.

3.2 Higher Order Sliding Mode Controller (HOSMC)

The proposed HOSMC controller named as Super Twisting Algorithm (STA) is an effective control algorithm for uncertain systems and it overcomes the main drawbacks of classical sliding mode controller described in Section 3.1.

Fig. 4 shows block diagram representation of higher order sliding mode control – Super Twisting Algorithm (STA) approach for Voltage Source Converter (VSC) in UPS application. Proportional Integral (PI) controller is used to reduce steady state errors in three phase output voltage waveform [17].

$$x_{error} = x_{ref} - x_{act}\,. \tag{31}$$

The sliding surface in case of HOSMC is taken as (32) where k is a sliding coefficient of the controller

$$s = x_{error} + k\frac{\mathrm{d}\,x_{error}}{\mathrm{d}\,t}\,. \tag{32}$$

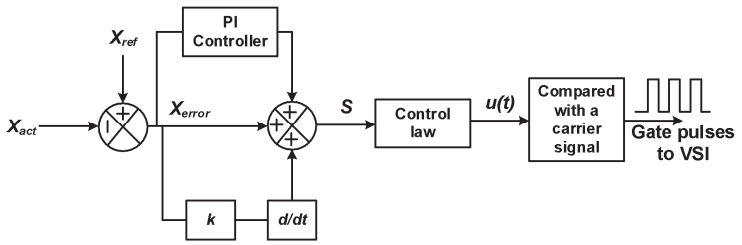

Fig. 4 – *STA control diagram.*

In SMC the control input applies on the first derivative of the sliding surface, but in STA it acts on the second order derivative of the sliding surface. The control input comprises of two inputs as (33)

$$u(t) = u_1 + u_2\,, \tag{33}$$

$$u_1 = -\lambda_1\sqrt{|s|}\,\mathrm{sign}(s)\,, \tag{34}$$

$$\dot{u}_2 = -\lambda_2 \operatorname{sign}(s)\,, \tag{35}$$

$$u_2 = \lambda_2 \int \operatorname{sign}(s)\,. \tag{36}$$

Substitute (34) and (35) in (33), then the control input of the STA is obtained as (37)

$$u(t) = -\lambda_1 \sqrt{|s|}\operatorname{sign}(s) - \lambda_2 \int \operatorname{sign}(s)\,, \tag{37}$$

where u_1 is continuous function of sliding surface and u_2 is discontinuous time derivative function of sliding surface. The tuning constants λ_1 and λ_2 are used to tune the STA to smoothen the controller. The modulus of sign function is to increase the life of the components of the VSC circuit. The integral term of the sign function resembles low pass filter characteristics [18]. The super twisting control law do not require the knowledge of S and it can be applied to system with relative degree one. Here VSI is a system with relative degree one and hence STA can be applied. Hence it can reduce or eliminate chattering problem.

This is the design process using STA for the UPS system.

3.2.1 Implementation of STA for three phase voltage source inverter

In HOSMC, only output load voltages are taken as state variables of a three phase voltage source inverter circuit. The Sinusoidal Pulse Width Modulation (SPWM) method is used to generate gate pulses to the IGBT switches. By using Clark transformation, transform three phase (*abc*) to two phase (αβ) co-ordinates. The errors of the output voltage variable are shown in (38)−(39),

$$v_{\alpha error} = v_{\alpha ref} - v_{\alpha act}\,, \tag{38}$$

$$v_{\beta error} = v_{\beta ref} - v_{\beta act}\,. \tag{39}$$

Correspondingly S_α and S_β are obtained as (40) and (41)

$$s_\alpha = \left(v_{\alpha error} + k_1 \frac{\mathrm{d}v_{\alpha error}}{\mathrm{d}t} \right) + \left(k_p + \frac{k_I}{s} \right), \tag{40}$$

$$s_\beta = \left(v_{\beta error} + k_2 \frac{\mathrm{d}v_{\beta error}}{\mathrm{d}t} \right) + \left(k_p + \frac{k_I}{s} \right). \tag{41}$$

The control inputs are obtained from (42)

$$\begin{aligned} u_a &= -\lambda_1 \sqrt{|s_a|}\operatorname{sign}(s_a) - \lambda_2 \int \operatorname{sign}(s_a), \\ u_b &= -\lambda_1 \sqrt{|s_b|}\operatorname{sign}(s_b) - \lambda_2 \int \operatorname{sign}(s_b), \\ u_c &= -\lambda_1 \sqrt{|s_c|}\operatorname{sign}(s_c) - \lambda_2 \int \operatorname{sign}(s_c). \end{aligned} \tag{42}$$

The input control signals are compared with repetitive carrier waveforms to get IGBT gate switching pulses of the three phase voltage source inverter circuit.

3.2.2 Implementation of STA for Three Phase Controlled rectifier

For a rectifier, the controller consists of an inner current loop controller and outer voltage loop controller. The system input source currents (i_{as}, i_{bs}, i_{cs}) and output dc voltage (v_{dc}) are taken as state variables.

$$s_{dc} = v_{dcref} - v_{dc}\,, \tag{43}$$

$$i_{dref} = k_1(k_{pdc}s_{dc} + k_{idc}\int s_{dc}\,\mathrm{d}t)\,, \tag{44}$$

whereas k_1 using as a sliding coefficient for the controller. Considering here $i_{qref} = 0$ because the system effectively works under unity power factor operation.

$$\left.\begin{aligned} i_{derror} &= i_{dref} - i_d \\ i_{qerror} &= i_{qref} - i_q \end{aligned}\right\}, \tag{45}$$

$$\left.\begin{aligned} s_d &= i_{derror} + k_3\frac{\mathrm{d}i_{derror}}{\mathrm{d}t} \\ s_q &= i_{qerror} + k_4\frac{\mathrm{d}i_{qerror}}{\mathrm{d}t} \end{aligned}\right\}, \tag{46}$$

where k_3 and k_4 are the sliding coefficients of the controller

$$\left.\begin{aligned} u_d &= -\lambda_1\sqrt{|s_d|}\,\mathrm{sign}(s_d) - \lambda_2\int \mathrm{sign}(s_d) \\ u_q &= -\lambda_1\sqrt{|s_q|}\,\mathrm{sign}(s_q) - \lambda_2\int \mathrm{sign}(s_q) \end{aligned}\right\}. \tag{47}$$

The sliding surfaces shown in (46) are used as input to the STA control law. The STA is used to smooth disturbances occurring in sliding surface and it generates control inputs as shown in (47). Feed forward decoupling is implemented to make the control design easier using (48)

$$\left.\begin{aligned} e_d &= v_d - \omega L i_q - u_d \\ e_q &= v_q + \omega L i_d - u_q \end{aligned}\right\}. \tag{48}$$

The feed forward decoupling control strategy is used to produce the control signals i.e. compared with triangular signal it creates the pulses to IGBT switches of the three phase controlled rectifier.

This design process is implemented for a UPS system based on STA to obtain a pure sinusoidal waveform and to reduce chattering phenomenon. The controllers block diagram for HOSMC for the rectifier side and VSI of the UPS system are presented in Fig. 5 which follows the design equations presented in Section 3. 2.1 and 3.2.2 respectively.

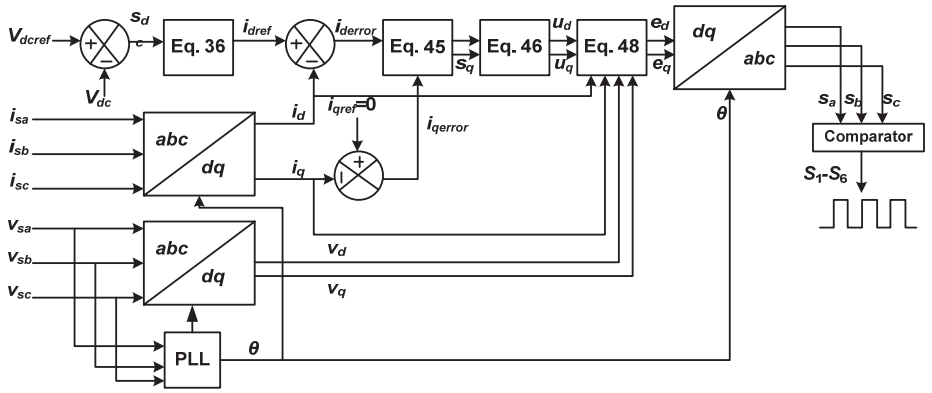

(a)

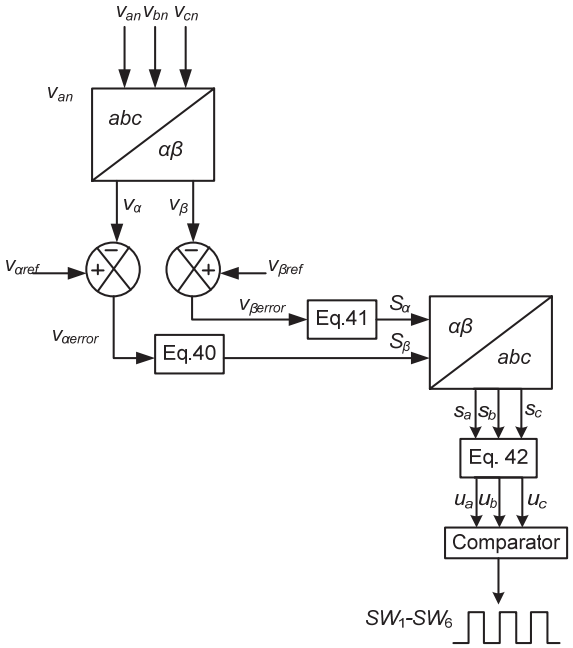

(b)

Fig. 5 – *HOSMC Control block diagrams used in UPS for* (a) *rectifier;* (b) *VSI.*

3.3. Enhanced Exponential Reaching Law (EERL-SMC)

Fig. 6a shows the control algorithm of EERL-SMC. Fig. 6b shows the locus of the reaching time in SMC and EERL-SMC.

$$\sigma_s = k_1(x_{ref} - x_{act}) + k_2(y_{ref} - y_{act}), \tag{49}$$

$$\sigma_s = k_1 \times x_{error} + k_2 \times y_{error}. \tag{50}$$

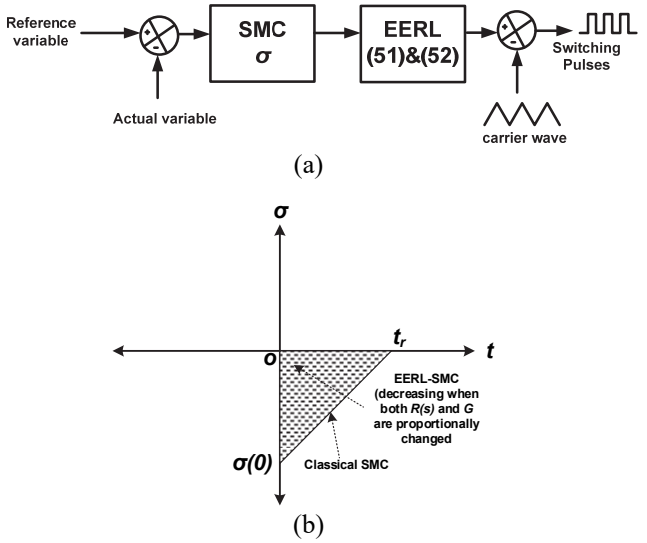

Fig. 6 − (a) *Simplified Control Block Diagram of EERL-SMC;*
(b) *Comparison of Reaching time for SMC and EERL-SMC.*

The proposed enhanced exponential reaching law completely eliminates the chattering problem and is more robust against sudden change in load and line variations [19]. The state variable error reaching to origin takes less time period. The EERL is defined as (51) where

$$\dot{\sigma} = -A\sigma_s - \left(\frac{G}{R(s)} \left| \sigma_S \right|^{\gamma} \operatorname{sgn}(\sigma_s) \right), \tag{51}$$

$$R(s) = \alpha + ((1-\alpha)e^{-\beta|\sigma_s|}) > 0\,. \tag{52}$$

A, G, $\beta > 0$ are positive integers; $0 < \alpha < 1$ and $0 < \gamma < 1$ are also positive integers. *R(s)* is always positive at all times; hence it has no effect on the stability of the SMC [20 − 23]. **Table 2** shows the system performance to controller parameter variations. The reaching time t_r for a first order SMC is given by $t_r = |\sigma(0)|/\lambda$ and the reaching time for exponential reaching law is given by $t_r = \frac{1}{G}\left(\alpha|\sigma_s| + \frac{(1-\alpha)}{\beta_x}\left[1 - e^{-\beta_x|\sigma_s|}\right] \right)$ [24].

Fig. 6b shows the EERL-SMC manipulates the system states whenever modulus of σ is very high or very small. Therefore it reduces the settling time and diminishes chattering whenever it is close to the sliding surface σ. This algorithm is used for the voltage control in a UPS system which produces a pure sine wave with less THD. The methodology is the same for generating the inner current references and outer voltage references in the rectifier. For the VSI, the filter inductor currents and loads voltages references are generated using (53).

$$\left.\begin{aligned} i_{\alpha ref} &= v_{\alpha error}(k_{p\alpha} + k_{i\alpha}/s) \\ i_{\beta ref} &= v_{\beta error}(k_{p\beta} + k_{i\beta}/s) \end{aligned}\right\}. \tag{53}$$

These are inputs to the EERL algorithm as shown in Fig. 6a.

Table 2
System performance for parametric variations.

Parameter	Observation
A (*Base value* 2000) $1000 < A < 3500$	Whenever this controlled parameter is increased the V_{THD} (%) in voltage increases but output voltage steady state error decreases. Whenever this controlled parameter is decreased the V_{THD} (%) in voltage is decreased but output voltage steady state error increases.
G (*Base value* 10) $5 < G < 20$	Whenever this controlled parameter is increased (or) decreased the percentage of V_{THD} in voltage doesn't change but steady state error of the output voltage increases.
β (*Base value* 0.5) $0.2 < \beta < 2$	Whenever this controlled parameter also increased (or) decreased the percentage of V_{THD} (%) in voltage doesn't change but steady state error of the output voltage increases.

Accordingly the switching pulses are produced to the IGBT switches of the VSI circuit. The stability is analysed using the Lyapunov criterion (30).

4 Working of a Buck/Boost Converter

The design of closed loop controller for dc/dc buck/boost converter for battery bank is based on the following algorithm.

$$p_{grid} > p_{Load}, \quad \begin{aligned} S_{buck} &= \text{ON} \\ S_{boost} &= \text{OFF} \end{aligned} \tag{54}$$

$$p_{grid} < p_{Load}, \quad \begin{aligned} S_{buck} &= \text{OFF} \\ S_{boost} &= \text{ON} \end{aligned} \tag{55}$$

S_{buck} is ON, when the battery is in charging mode and S_{boost} is ON, when the battery is in the discharging mode. Therefore the switching signals to the switches of converter are generated based on whether battery needs to be charged or discharged. **Table 3** shows the battery specifications used in this work.

Table 3
Specifications of Battery.

Parameters	Values
Battery Rating	41.6 AH
Nominal Voltage	400 V
Nominal Discharge Current	20%

5 Analysis and Simulation Results

Table 4 shows the specifications of the 30kVA UPS inverter working at a frequency of 50Hz. The parameters for EERL-SMC are shown in **Table 2**. Simulation results of EERL-SMC have been presented here to validate the controllers performance to reach the origin i.e. achieve stability in minimum time i. e. less settling time. Fig.7 shows a three phase rectifier input source voltage and current for only one phase represented on a single graph when resistive load is connected. Power factor of the system is near to unity.

Table 4

Specifications of UPS System.

Parameters	Values
UPS system rating	30 kVA/415 V/50Hz
DC link voltage (V_{dcref})	850 V
Switching Frequency	10 kHz
Input source & output load filter inductance Output load capacitive filter	1 mH 0.23mF
Loads	Linear load=10 kW,0.8 pf lag and Non-linear load i.e. 3-Ø DBR
Sliding Coefficients	k_1=280, k_2= 25

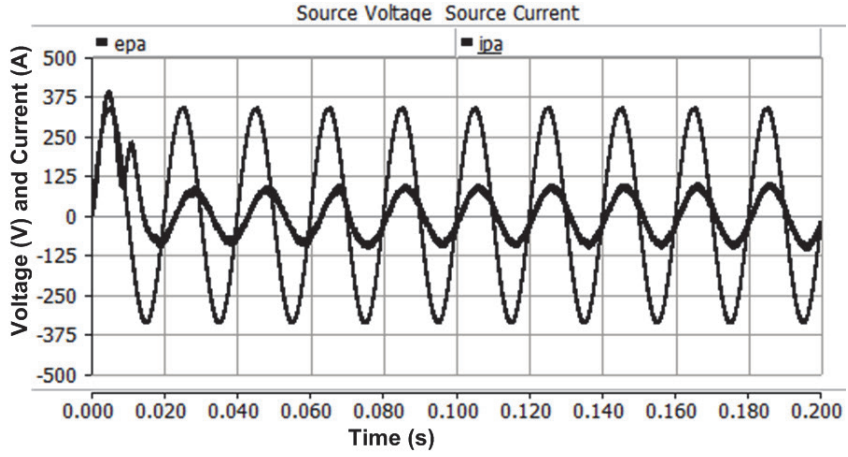

Fig. 7 – *Input source voltage and current of a controlled rectifier for one phase.*

Fig. 8 shows three phase-controlled rectifier output DC voltage (v_{dcref} = 850 V). When battery is in charging mode, the output dc voltage is less than the reference value and during discharging mode; it is tracking the reference value of 850 V.

Fig. 9 shows the switching pulses for the switches in buck/boost converter, during charging and discharging states of the battery.

Fig. 10 shows battery State of Charge conditions (SOC). During power supply, buck converter is ON and the battery is in charging mode. During loss of power supply, boost converter is ON and the battery is in discharging mode of operation.

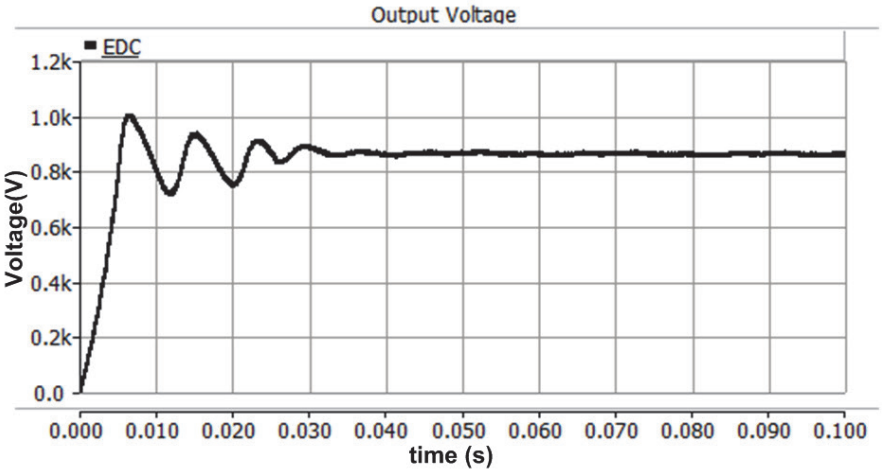

Fig. 8 – *Output DC voltage of controlled rectifier.*

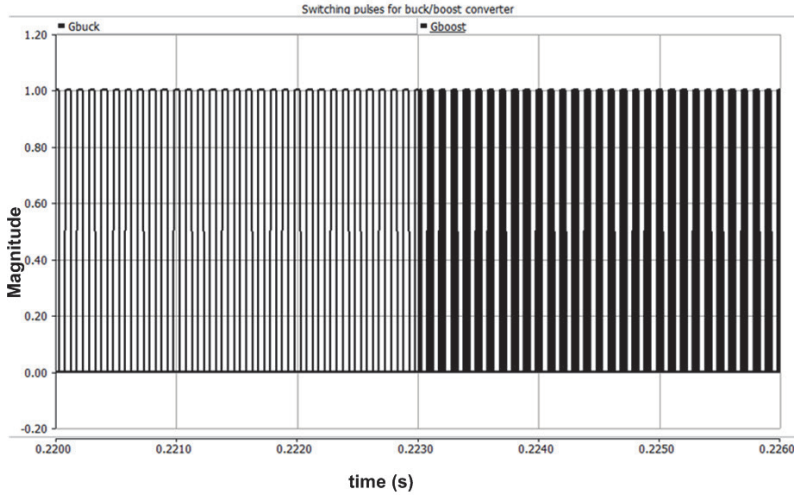

Fig. 9 – *Switching pulses for Buck/Boost converter.*

Fig. 11 shows the EERL-SMC sliding surface of 1v (p-p) and from Fig. 12, it is observed the dynamic response of the controller for a change in load from 15 kW to 25 kW at t =1.2 s to 1.3 s and again sudden change from 15 kW to 22.5 kW at t =1.4 s to t =1.5 s.

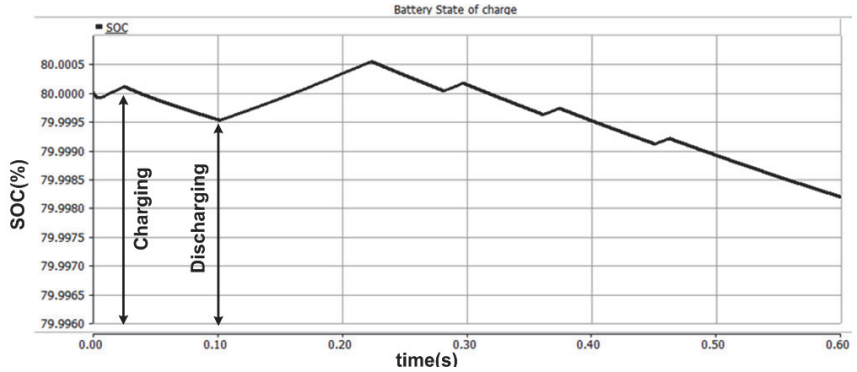

Fig. 10 – *Battery state of charge conditions.*

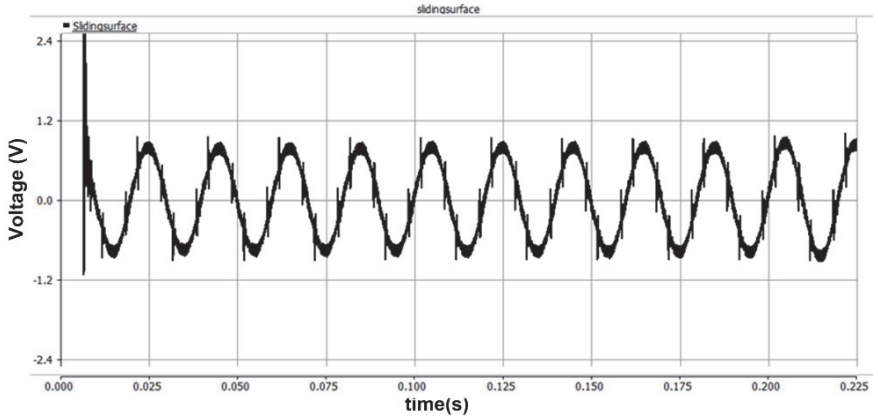

Fig. 11 – *Sliding surface of sliding mode controller.*

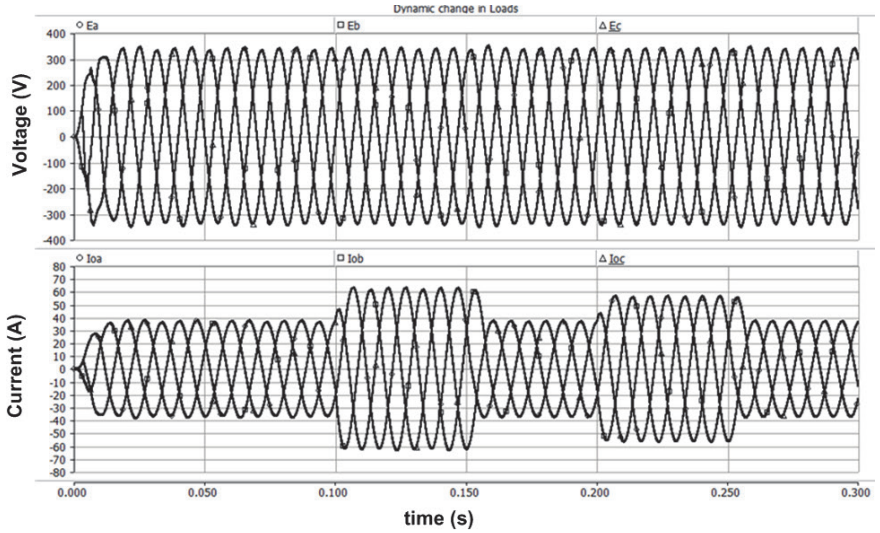

Fig. 12 – *Dynamic change in load conditions.*

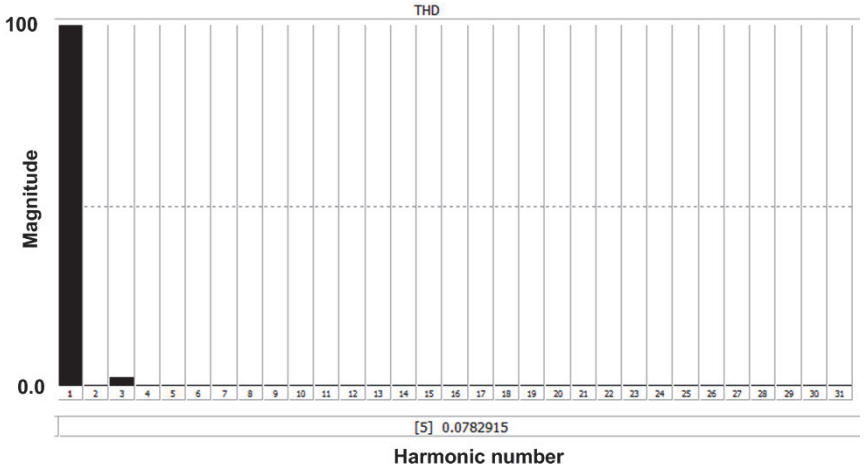

Fig. 13 – *Harmonic spectrum of load voltage for linear load.*

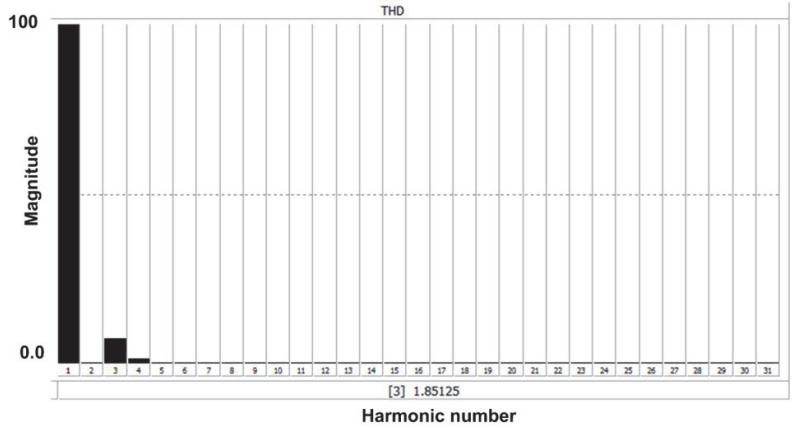

Fig. 14 – *Harmonic spectrum of load voltage for non-linear load.*

Fig. 15 shows the voltage error in EERL-SMC is 1000 times less than that in SMC which clearly states that the proposed controller works well in reducing the steady state error. The settling time is observed to be 4 ms in case of EERL-SMC while it is 10 ms in SMC. The simulations are performed with the same parameters for SMC, HOSMC and EERL-SMC for more understanding.

It therefore confirms that EERL based SMC is fast and accurate.

Fig. 16 shows the tracking of the reference output phase voltage v_{ref} to the actual output phase voltage $v_{act.}$ in SMC, HOSMC and EERL-SMC. It is clear that the proposed controller well tracks effectively with very less steady state error. It is 10V in SMC, 6V in HOSMC and 4V in EERL-SMC. Hence the controller is said to possess good tracking capability.

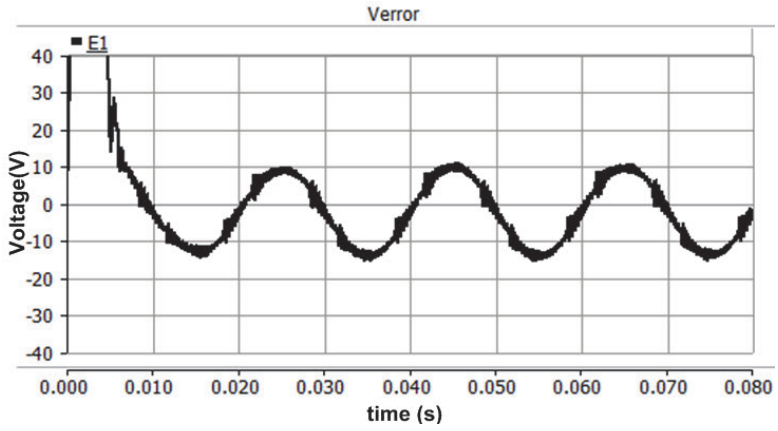

(a)

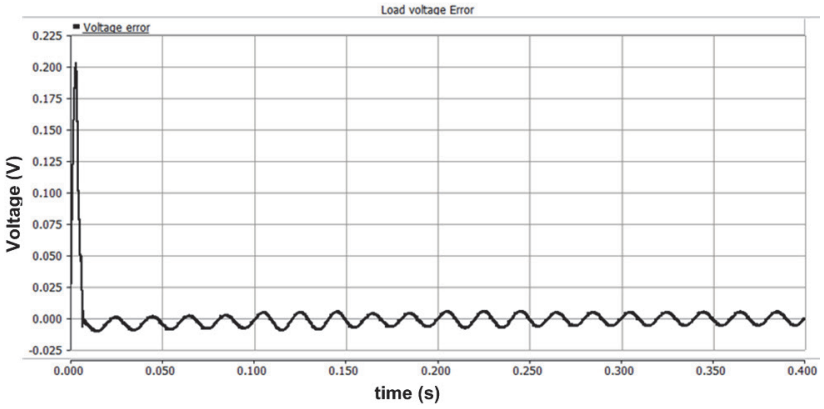

(b)

Fig. 15 – *Load voltage error* (a) *SMC;* (b) *EERL-SMC.*

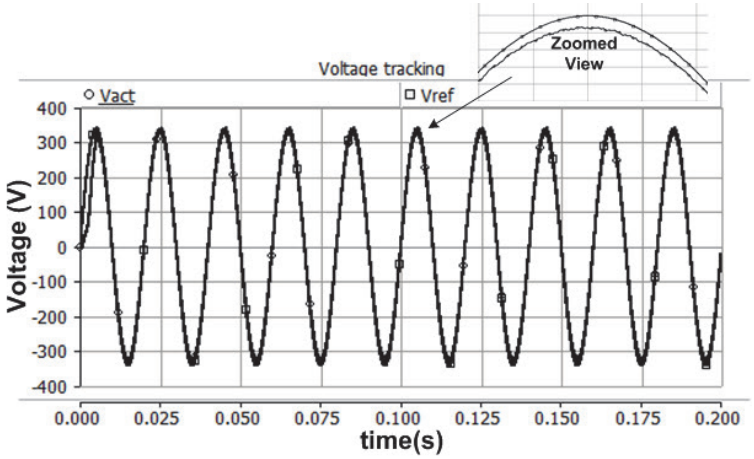

Fig. 16a – *Phase voltage tracking: SMC.*

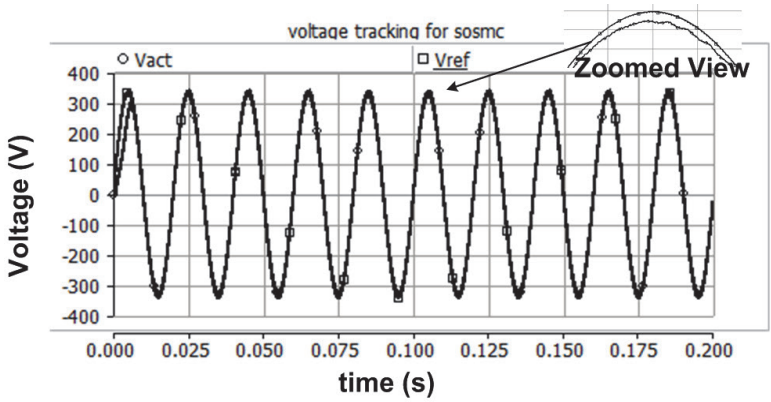

(b)

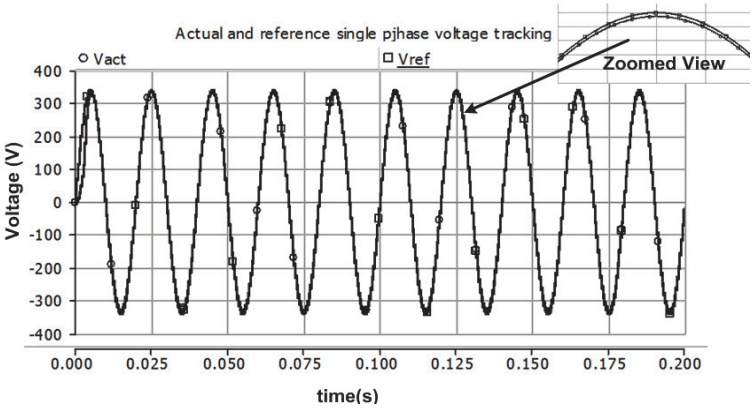

(c)

Fig. 16 − *Phase voltage tracking:* (b) *HOSMC;* (c) *EERL-SMC.*

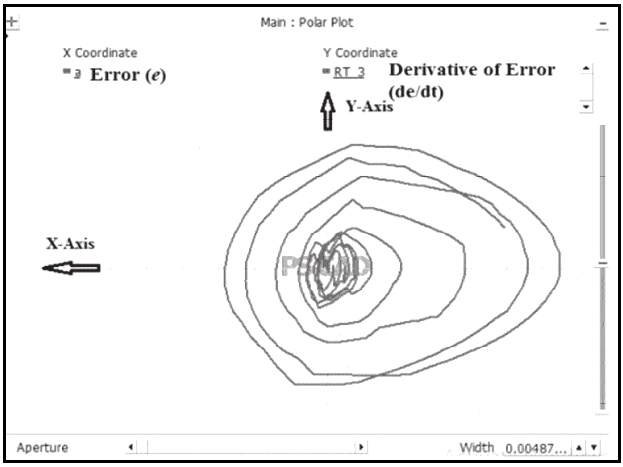

Fig. 17a − *Phase Plane trajectory of SMC.*

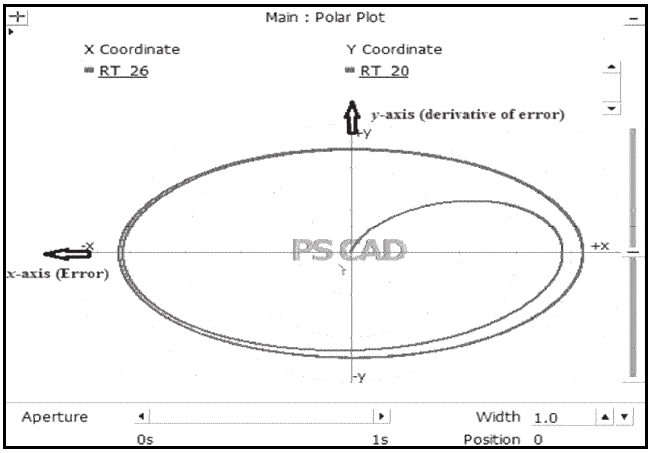

Fig. 17b – *Phase Plane trajectory of HOSMC.*

Figs. 17a and 17b show the state variable i.e. the output voltage is able to reach the origin from its unstable state in the phase plane in a very short period. Compared to SMC HOSMC is better in regulating the high frequency oscillations associated during the controllers operation. Fig. 18 shows the shows a phase plane trajectory view of EERL-SMC. The chattering problem in the system is completely eliminated by using proposed Enhanced Exponential Reaching Law.

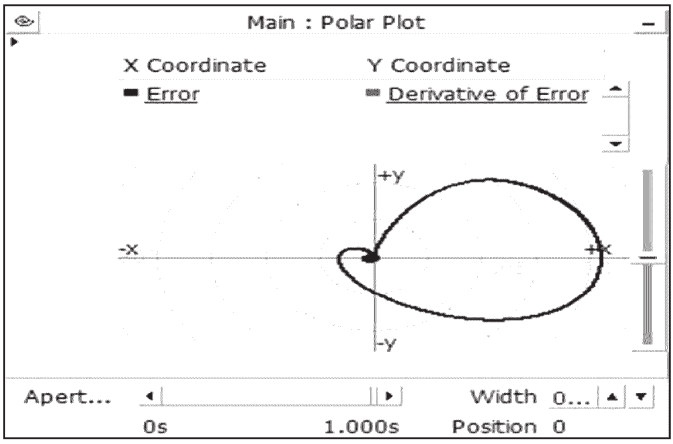

Fig. 18 – *Phase Plane trajectory view of EERL-SMC.*

It is clear that the THD obtained in output voltage is very less compared to that obtained in SMC and HOSMC. Also steady state error (voltage regulation) and settling time observed using this algorithm is 1.74 % and 4ms. The dynamic nature of the proposed algorithm is good in obtaining a sinusoidal output

voltage waveform. Hence this controller can be adapted in place of HOSMC for obtaining a better voltage waveform for critical loads.

Table 5
Comparison of EERL-SMC with HOSMC and SMC.

Type of load connected at PCC	% Voltage THD		
	Conrol Algorithm		
	SMC	HOSMC	EERL-SMC
Linear Load	0.91	0.14	0.12
Non-Linear Load	1.14	0.28	0.18

5 Conclusion and Future Scope

The work addresses an enhanced exponential reaching law (EERL) based SMC EERL-SMC for a three phase UPS system used in industrial applications. A DC-DC Buck/Boost switch is used for charging and discharging the battery during on grid and off grid conditions. The state space models of three phase rectifier, VSI are developed to realize the control parameters and stability. Mathematical [design] of SMC, HOSMC and the proposed EERL-SMC are discussed in detail for the UPS system. The controller is applied both on the rectifier side to regulate the DC voltage and also to the VSI to control the output voltage across the load. It is observed that this controller is robust with less steady state error and less settling time compared to a classical SMC and HOSMC. Good tracking capabilities of the desired variable, very fast steady state reaching speed, robust in dynamic nature of the controller and also elimination of chattering problem in SMC is realized. A phase plane plot has been shown to validate it. This controller can be an alternative to HOSMC. This controller suits to the UPS system connected to any critical load like the military and hospital systems where reliable power supply is very much essential. A comparison is brought out with respect to SMC and HOSMC in terms of chattering, tracking and output voltage THD for use of this algorithm for UPS systems. The work can be extended with fractional order sliding mode controllers (FOSMC) to obtain zero steady state error and zero settling time. Solar based UPS System can also be taken up as an extension of this work.

6 References

[1] P. S. Bimbhra: Power Electronics, 5th Edition, Khanna Publishers, New Delhi, 2012.

[2] V. Utkin: Variable Structure Systems with Sliding Modes, IEEE Transactions on Automatic Control, Vol. 22, No. 2, April 1977, pp. 212 – 222.

[3] S. K. Gudey, R. Gupta: Reduced State Feedback Sliding-Mode Current Control for Voltage Source Inverter-Based Higher-Order Circuit, IET Power Electronics, Vol. 8, No. 8, August 2015, pp. 1367 – 1376.

[4] S. K. Gudey, R. Gupta: Second Order Sliding Mode Control for a Single Phase Voltage Source Inverter, Proceedings of the IEEE Region 10 Conference (TENCON), Bangkok, Thailand, October 2014, pp. 1 – 6.

[5] X. Q. Guo, W. Y. Wu: Improved Current Regulation of Three-Phase Grid-Connected Voltage-Source Inverters for Distributed Generation Systems, IET Renewable Power Generation, Vol. 4, No. 2, March 2010, pp. 101 – 115.

[6] S. K. Gudey, R. Gupta: Sliding-Mode Control in Voltage Source Inverter-Based Higher-Order Circuits, International Journal of Electronics, Vol. 102, No. 4, July 2014, pp. 668 – 689.

[7] G. S. Rajan, H. N. Nagaraj: Comparison Between Sigmoid Variable Reaching Law and Exponential Reaching Law for Sliding Mode Controlled DC-DC Buck Converter, Proceedings of the International Conference on Power, Energy and Control (ICPEC), Sri Rangalatchum Dindigul, India, February 2013, pp. 316 – 319.

[8] Q.- N. Trinh, F.- H. Choo, J. Chi, W. Peng: An Improved Control Strategy for Three-phase AC/DC/AC Converter in UPS Application, Proceedings of the Asian Conference on Energy Power and Transportation on Electrification (ACEPT), Singapore, Singapore, October 2016, pp. 1 – 6.

[9] A. Bouzidi, M. L. Bendaas, S. Barkat, M. Bouzidi: Sliding Mode Control of Three-Level NPC Inverter Based Grid-Connected Photovoltaic System, Proceedings of the 6th International Conference on Systems and Control (ICSC), Batna, Algeria, May 2017, pp. 354 – 359.

[10] M. Bani Shamseh, A. Kawamura, T. Yoshino: A Novel Autonomous Control Scheme for Parallel, LCL-Based UPS Systems, Proceedings of the IEEE Energy Conversion Congress and Exposition (ECCE), Milwaukee, USA, September 2016, pp. 1 – 8.

[11] B. Sudhakar, G. V. E. Satish Kumar: Co-simulation of Sliding Mode Control of Single Phase Grid Connected LCL Filtered Voltage Source Inverter Using Lab VIEW and Multisim, Proceedings of the IEEE Region 10 Conference (TENCON), Singapore, Singapore, November 2016, pp. 311 – 315.

[12] B. Bhutia, S. M. Ali, N. Tiadi: Design of Three-Phase PWM Voltage Source Inverter for Photovoltaic Application, International Journal of Innovative Research in Electrical, Electronics, Instrumentation and Control Engineering, Vol. 2, No. 4, April 2014, pp. 1364 – 1367.

[13] S. A. Lakshmanan, B. S. Rajpourhit, A. Jain: Modelling and Analysis of 3-Phase VSI Using SPWM Technique for Grid Connected Solar PV system, Proceedings of the IEEE Students' Conference on Electrical, Electronics and Computer Science, Bhopal, India, March 2014, pp. 1 – 6.

[14] H. Komurcugil, N. Altin, S. Ozdemir, I. Sefa: Sliding-Mode and Proportional-Resonant Based Control Strategy for Three-Phase Grid-Connected LCL-Filtered VSI, Proceedings of the 42nd Annual Conference of the IEEE Industrial Electronics Society, Florence, Italy, October 2016, pp. 316 – 319.

[15] M. M. Alhato, S. Bouallegue, M. Ayadi: Modeling and Control of an AC-DC Voltage Source Converter based on Sliding Mode and Fuzzy Gain-Scheduling Approaches, Proceedings of the 7th International Conference on Sciences of Electronics, Technologies of Information and Telecommunications (SETIT), Hammamet, Tunisia, December 2016, pp. 332 – 337.

[16] Z. Zhang, X. Liu, C. Liu, J. Ming, L. Yang: Sliding Mode and Feedback Linearization Control of Three Phase Voltage Source PWM Converter, Proceedings of the 35th Chinese Control Conference (CCC), Chengdu, China, July 2016, pp. 8666 – 8670.

[17] M. Cucuzzella, G. P. Incremona, A. Ferrara: Design of Robust Higher Order Sliding Mode Control for Microgrids, IEEE Journal on Emerging and Selected Topics in Circuits and Systems, Vol. 5, No. 3, September 2015, pp. 393 – 401.

[18] V. Naik, S. K. Gudey, A. R. Anuku: Design of Robust Feedback Controller for a UPS System in Industrial Application, Proceedings of the Recent Advances on Engineering, Technology and Computational Sciences (RAETCS), Allahabad, India, February 2018, pp. 1 – 6.

[19] H. Ma, J. Wu, Z. Xiong: A Novel Exponential Reaching Law of Discrete-Time Sliding-Mode Control, IEEE Transactions on Industrial Electronics, Vol. 64, No. 5, May 2017, pp. 3840 – 3850.

[20] S. Su, H. Wang, H. Zhang, Y. Liang, W. Xiong: Reducing Chattering Using Adaptive Exponential Reaching Law, Proceedings of the 6th International Conference on Natural Computation (ICNC), Yantai, China, August 2010, pp. 3213 – 3216.

[21] S. M. Mozayan, M. Saad, H. Vahedi, H. Fortin-Blanchette, M. Soltani: Sliding Mode Control of PMSM Wind Turbine based on Enhanced Exponential Reaching Law, IEEE Transactions on Industrial Electronics, Vol. 63, No. 10, October 2016, pp. 6148 – 6159.

[22] Z. Yin, Y. Zhang, X. Tong, Y. Zhong: Model Predictive Control Using Globe Exponential Reaching Law Sliding Mode Design Method for Induction Motor Drives, Proceedings of the IEEE Applied Power Electronics Conference and Exposition (APEC), Anaheim, USA, March 2019, pp. 2559 – 2563.

[23] K. B. Devika, S. Thomas: Improved Sliding Mode Controller Performance Through Power Rate Exponential Reaching Law, Proceedings of the 2nd International Conference on Electrical, Computer and Communication Technologies (ICECCT), Coimbatore, India, February 2017, pp. 1 – 7.

[24] V. K. Nagaboina, S. K. Gudey: Design and Analysis of a Three Phase Transformerless Hybrid Series Active Power Filter based on Sliding Mode Control Using PQ- Theory and Stationary Reference Frames, Serbian Journal of Electrical Engineering, Vol. 16, No. 3, October 2019, pp. 289 – 310.